LANGMUIR

Article

pubs.acs.org/Langmuir

Identification of ROS Produced by Nanobubbles and Their Positive and Negative Effects on Vegetable Seed Germination

Shu Liu,*[,†] Seiichi Oshita,*[,†] Saneyuki Kawabata,[†] Yoshio Makino,[†] and Takahiko Yoshimoto[†]

[†]Graduate School of Agricultural & Life Sciences, The University of Tokyo, Yayoi 1-1-1, Bunkyo-ku, Tokyo 113-8657, Japan

Supporting Information

ABSTRACT: Exogenous reactive oxygen species (ROS) produced by nanobubble (NB) water offer a reasonable explanation for NBs' physiological promotion and oxidation effects. To develop and exploit the NB technology, we have performed further research to identify the specific ROS produced by NBs. Using a fluorescent reagent APF, a Fenton reaction, a dismutation reaction of superoxide dismutase and DMSO, we distinguished four types of ROS (superoxide anion radical ($O_2\cdot^-$), hydrogen peroxide (H_2O_2), hydroxyl radical (·OH), and singlet oxygen ($^1O_2$)). ·OH was confirmed to be the specific ROS produced by NB water. The role of ·OH produced by NB water in physiological processes depends on its concentration. The amount of exogenous ·OH has a positive correlation with the NB number density in the water. Here, spinach and carrot seed germination tests were repeatedly performed with three seed groups submerged in distilled water, high-number density NB water, and low-number density NB water under similar dissolved oxygen concentrations. The final germination rates of spinach seeds in distilled water, low-number density NB water, and high-number density NB water were 54%, 65%, and 69%, respectively. NBs can also promote sprout growth. The sprout lengths of spinach seeds dipped in NB water were longer than those in the distilled water. For carrot seeds, the amount of exogenous ·OH in high-number density NB water was beyond their toxic threshold, and negative effects were shown on hypocotyl elongation and chlorophyll formation. The presented results allow us to obtain a deeper understanding of the physiological promotion effects of NBs.

INTRODUCTION

Reactive oxygen species (ROS) have historically been viewed as purely harmful metabolic byproducts that cause oxidative damage to lipids, proteins, and nucleic acid.[1] Research in recent decades, however, has highlighted new roles for ROS as important physiological regulators of cellular signaling pathways. The concept of a "biological window" or an "oxidative window" was raised in the fields of both plant biology and health and medicine.[2,3] Too few ROS may result in decreased antimicrobial defense, whereas too many ROS could destroy cells and produce pathological effects; however, a moderate level of ROS will play a positive role in growth.[2,4] Both endogenous and exogenous sources contribute to the formation of intracellular ROS.[5] Endogenous sources of cellular ROS include NADPH oxidase, mitochondrial oxidant, cytochrome c oxidase, and xanthine oxidase.[6] Exogenous sources include irradiation (UV, X-, and γ-rays)[5] and chemicals such as exogenous H_2O_2.[7−9]

In recent decades, many papers have presented case studies on the effects of micro and nanobubbles (MNBs) on the physiological activity of living organisms, such as promoting the growth of plants,[10,11] fish,[12−14] and cell cultures.[15,16] Although some reports have attempted to describe the reason for which physiological activity is promoted, most have simply represented case studies without elaborating the mechanisms. Recently, a new characteristic of NBs was discovered by our research group, namely, that without any stimuli, NB water could continually produce small amounts of ROS in the water using a sensitive fluorescent probe, 3′-*p*-(aminophenyl) fluorescein (APF).[17] In the same year, Minamikawa et al. reported that using electron spin resonance (ESR) spectra, free radicals were likely to be generated by the collapse of NBs.[18] The generation of ROS due to NBs offered a reasonable explanation for the physiological promotion effect of NBs. However, ROS are not single entities but represent a broad range of chemically distinct reactive species with diverse biological reactivities.[19] Therefore, to develop and exploit the NB technology, further research must be performed to identify the types of ROS produced by NBs. The main types of ROS include the superoxide anion radical ($O_2\bullet^-$), hydrogen peroxide (H_2O_2), hydroxyl radical (•OH), and singlet oxygen ($^1O_2$), which are metabolic byproducts in both plants and animals.[20] Pure water is composed of two elements, hydrogen and oxygen; therefore, these four types of ROS are the most likely species to be produced in oxygen NB water. ESR has been widely used to detect the free radical generation by MNBs in the presence of dynamic stimuli such as ozone, strong acid, and copper.[21−23] However, the high DO concentration in oxygen NB water will affect the ESR spectra of free radicals in solution. As oxygen is paramagnetic, oxygen-radical collisions contribute to the magnetic relaxation of free radicals and cause subsequent

Special Issue: Nanobubbles

Received: April 28, 2016
Revised: June 2, 2016
Published: June 3, 2016

DOI: 10.1021/acs.langmuir.6b01621
Langmuir 2016, 32, 11295−11302

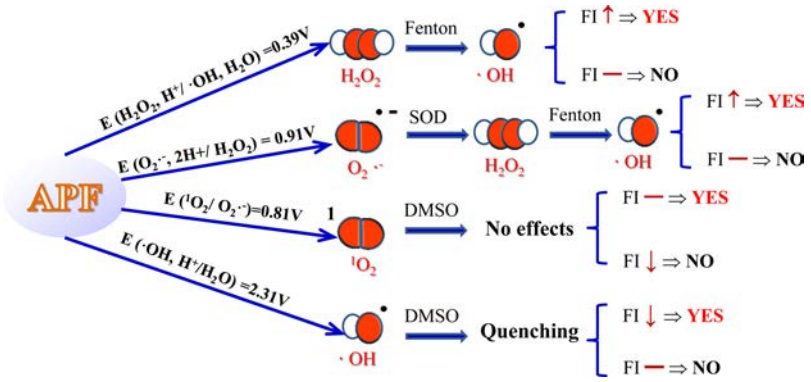

Figure 1. Schematic of experimental design for ROS identification (FI: Fluorescence intensity; ↑: increase; ↓: decrease; —: no change).

ESR line broadening.[24] Meanwhile, using the ESR method, some researchers have observed free radical generation by NB water itself,[18] whereas some did not.[25] For the above reasons, an alternative higher sensitivity methodology is needed for detection of the production small quantities of ROS by NB water itself without any stimuli. The fluorescence methodology, associated with the use of suitable probes, is an excellent approach to measure ROS because of its high sensitivity, simplicity in data collection, and high spatial resolution in microscopic imaging techniques.[26] Thus, in this paper we try to identify what type of ROS is produced by NB water using a fluorescent probe, APF. A strong oxidizing power is required for the ipso-substitution reaction of APF. Therefore, due to the different oxidizing powers of various ROS, the fluorescence responses of APF to them also differ. Based on the above fact, we can build a set of methods to distinguish the four types of ROS using APF and identify the specific type of ROS produced by oxygen NB water.

ROS are a double-edged sword. A moderate increase in ROS concentration may promote cell proliferation and survival. However, when ROS concentration reaches the toxic threshold, it may overwhelm the cellular antioxidant capacity and trigger the cell death process. Therefore, as signal molecules, different amounts of exogenous ROS produced by NBs will have different effects on the growth of living organisms. Furthermore, the amount of exogenous ROS positively correlated with the NB number density in the water.[17] Here, we study the effects of NB number density on the germination processes of two types of vegetable seeds (spinach and carrot). The germination rates and the elongation of roots and hypocotyls are both compared among the seeds submerged in water with different NB number densities. We intend to obtain a deeper understanding of the mechanism behind the physiological promotion effects of NBs, together with the identification of the ROS generated by them.

EXPERIMENTAL SECTION

Experimental Design. Figure 1 shows a schematic of ROS identification. The fluorescence response of APF to four different types of ROS will be studied. Due to the different oxidative capacities of ROS, which are related to electrode potential, the fluorescence responses should be different. First, we will try to identify whether the ROS produced by NBs is H_2O_2. The formation of •OH by a Fenton reaction will cause a dramatic increase in the fluorescence intensity. Therefore, if this phenomenon is not observed after adding ferrous ions to the H_2O_2 solution, the existence of H_2O_2 will be excluded. Second, we will try to identify whether the ROS produced by NBs is $O_2^{\bullet-}$. The dismutation of $O_2^{\bullet-}$ catalytic with superoxide dismutase (SOD) will lead to the formation of H_2O_2. Then, we will add ferrous ions to the solution. The ferrous ions would react with H_2O_2 to produce •OH, causing a dramatic increase in fluorescence intensity. If the fluorescence intensity of samples does not dramatically increase, the existence of $O_2^{\bullet-}$ will be excluded. Third, we will try to identify whether the ROS produced by NB water is •OH or $^1O_2$. DMSO is known to quench •OH but not $^1O_2$. Hence, after DMSO is added, if the fluorescence intensity of NB water decreases, the ROS will be •OH. Otherwise, the ROS will be $^1O_2$. More detail is provided in the Results and Discussion section.

Reagents. APF (5 mM, Sekisui Medical Co., Ltd., Japan), a fluorescent reagent that is highly resistant to autoxidation, was used to identify the different ROS. APF itself has almost no fluorescence intensity. After APF reacts with ROS, fluorescein (with strong fluorescence intensity) is generated. SOD (Bovine Erythrocytes 5612U/mg) was obtained from Nacalai Tesque Inc. Japan. Ultrapure water (1 mL) was added in 3000 units of SOD powder and the solution was used within 2 days. H_2O_2 (30%, Kanto Chemical Co., Inc., Japan) is prepared prior to each use. Other chemicals were purchased from Kanto Chemical Co., Inc., Japan and were of the highest obtainable purity.

Fluorescence Spectrophotometry. To obtain fluorescence excitation−emission matrices, the excitation wavelength was increased from 450 to 550 nm in 1 nm steps; for each excitation wavelength, the emission at longer wavelengths was also detected in 1 nm steps with a fluorescence spectrophotometer (F-7000, Hitachi High-Tech Co. Ltd., Japan). The slit width was 5 nm for both excitation and emission. The photomultiplier voltage was set to 700 V. Because the baseline fluorescence varies from probe to probe and from experiment to experiment, the fluorescence intensity was given as a relative value corresponding to a combination of parameters such as slit width, location of lamp, and voltage.[27] The fluorescein caused by ROS had an excitation−emission matrix peak located at an excitation wavelength of 490 nm and an emission wavelength of 515 nm.

Hydroxyl Radical Formation. Hydroxyl radical was generated by the well-known Fenton reaction.[28] Ferrous iron(II) is oxidized by H_2O_2 to ferric iron(III), a hydroxyl radical, and a hydroxyl anion, which is shown in eq 1. H_2O_2 of 0.1 mM was added to the sodium phosphate buffer (0.1 M, pH 7.4) containing APF and then various amounts of ferrous sulfate solutions were added. The final theoretical concentrations of •OH were in the range 0−25 μM. Ferrous sulfate solution was freshly prepared prior to each use.

Superoxide Anion Radical Formation. Reactions with potassium superoxide (KO_2) were performed during conditions of very low relative humidity. KO_2 powder was carefully weighed in dry beakers before use. Buffer solution containing APF was added with vigorous mixing in the beaker containing KO_2 powder. After reacting with KO_2 for 2 min, the fluorescence intensity was determined. The final theoretical concentrations of KO_2 ranged from 0 to 1 mM.

Singlet Oxygen Formation. Singlet oxygen was formed by 3-(1,4-epidioxy-4-methyl-1, 4-dihydro-1-naphthyl) propionic acid (EP). EP powder was carefully weighed in dry beakers before use. Buffer solution containing APF (buffer containing 10% ethanol) was added

DOI: 10.1021/acs.langmuir.6b01621
Langmuir 2016, 32, 11295−11302

with vigorous mixing in the beaker containing the EP powder. The mixtures were stirred a 37 °C for 15 min. The final theoretical concentrations of singlet oxygen ranged from 0 to 250 μM.

Fluorescence Intensity of NB Water. Pure oxygen (purity 99.99995%, Taiyo Nippon Sanso Co. Ltd., Japan) was introduced into a 2-L phosphate buffer (0.1 M, pH 7.4) and circulated through an MNB generator (OM4-GP-040, Aura Tec Co. Ltd., Japan) for 1 h at a constant temperature of 20 °C to obtain "oxygen NB water." The DO concentration of oxygen NB water was above 40 mg L^{-1}. APF of 2 μL was added into 10 mL of water containing NBs and the fluorescence intensities were measured. This was repeated more than five times. The final concentration of APF was 1 μM.

Seed Germination. Seeds of carrot (*Daucus carota subsp. sativus*) and spinach (*S. oleracea L.*), which were harvested in 2015 and stored under controlled conditions (room temperature), were obtained from Takii & Co. Ltd.

Germination tests were repeatedly performed with three seed groups. Each group was composed of 50 seeds. We used distilled water as a control. The DO concentration of distilled water was about 8 ppm. For NB water, a mixture of nitrogen and air was used to adjust the DO of MNB water to be the same as that of the distilled water. NB water was prepared following the method described in our previous paper.[17] To study the effect of NB number density on the germination process, we diluted NB water with distilled water in order to adjust the number density to be 20% of the original value. The original NB water is termed "100% NB water." The total NB number densities in control water, 100% NB water, and 20% NB water were about 0, 1.22×10^8, and 2.44×10^7 particles/mL, respectively (Supplemental data 1). NB number densities were measured using the nanoparticle tracking analysis method (NanoSight-LM10, Quantum Design Inc., Japan). The nanoparticle tracking analysis cannot distinguish between NBs and foreign matters. However, the decrease of total particle number density with storage time proved that most of the particles that exist in the water are actually NBs rather than solid nanoparticles.[11,17]

Spinach and carrot seeds were submerged in beakers filled with distilled water, 20% NB water, and 100% NB water in a ratio of 10 mL of water per seed. During the germination experiments, to avoid the lack of oxygen and to maintain a certain amount of NBs in the water, the 100% NB water, distilled water, and 20% NB water were changed twice a day. Germination tests for spinach and carrot seeds lasted for about 7 and 14 days, respectively.

Chlorophyll Content. Twenty carrot seeds were ground to fine powder with liquid nitrogen in a mortar and pestle and transferred to 2 mL tubes. Acetone solution (80%) of 500 μL was added to each tube and the contents were mixed, homogenized, and incubated at 4 °C in the dark for 2 h. Homogenates were clarified by centrifugation at 15 000 rpm for 10 min at 4 °C. Clarified extracts were used for chlorophyll content analyses. The absorption of the extracts was measured with a spectrophotometer by considering the spectrum between 500 and 700 nm. The absorption at 652 nm is used to represent the total chlorophyll content.

RESULTS AND DISCUSSION

Ground-state oxygen may be converted into ROS by energy- or electron-transfer reactions.[6] Energy transfer leads to the formation of $^1O_2$, whereas the successive one-electron reduction of molecular oxygen yields $O_2^{\bullet-}$, H_2O_2, •OH, and water. Each ROS has a characteristic oxidative capacity and a specific role in living cells. Based on the above, we tried to identify the certain type of ROS produced by NB water through the reactivity of APF with •OH, $O_2^{\bullet-}$, H_2O_2, and $^1O_2$.

Fluorescence Response of APF to Different Types of ROS. We compared the fluorescence responses of APF to •OH, $O_2^{\bullet-}$, H_2O_2, and $^1O_2$. From Figure 2, we can see the relationship between the fluorescence increases of APF with different concentrations of ROS. As shown in Figure 2a, the fluorescence increase of APF was proportional to the concentration of •OH. The •OH was formed from the Fenton reaction. Ferrous sulfate was added at various concentrations (1−25 μM) into the buffer solution of APF containing an excess of H_2O_2 (0.1 mM). According to the Fenton reaction shown in eq 1, ferrous iron(II) is oxidized by H_2O_2 into ferric iron(III), a hydroxyl anion, and a hydroxyl radical. The concentration of ferrous iron is equal to the concentration of the hydroxyl radical:

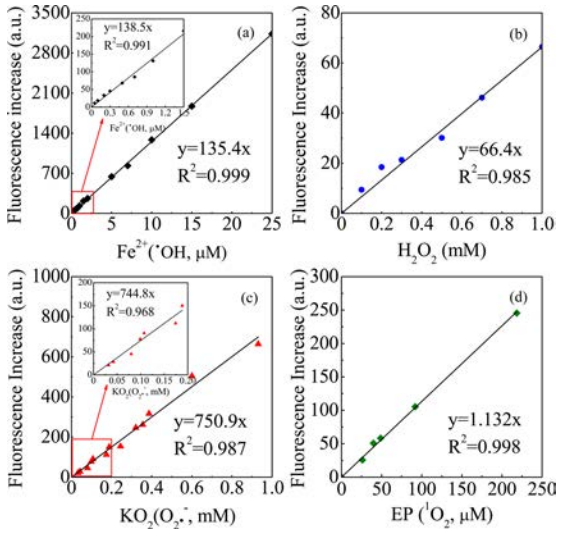

Figure 2. Fluorescence response of APF (0.1 M, pH 7.4) to different kinds of ROS. The fluorescence intensity was determined at 515 nm with excitation at 490 nm (a) Detection of •OH in the Fenton reaction (In the horizontal axis, the concentration of Ferrous iron(II) is equal to that of hydroxyl radicals, H_2O_2 (0.1 mM) was added to buffer solution of APF and then ferrous sulfate was added. The fluorescence increases were the fluorescence intensities minus the baseline signal obtained after adding 0.1 mM H_2O_2). (b) Fluorescence increase of APF in H_2O_2 system. (c) Fluorescence increase of APF in KO_2 system. (d) Fluorescence increase of APF in EP system. The fluorescence increases were the fluorescence intensities minus the baseline signal.

$$Fe^{2+} + H_2O_2 \rightarrow Fe^{3+} + OH^- + \bullet OH \quad (1)$$

Figure 2b shows the relationship between the fluorescence increase of APF and the concentration of H_2O_2. In the range of low H_2O_2 concentrations (0−1 mM), APF can be used to detect the existence of H_2O_2 in terms of a dose-dependent increase of fluorescence. By comparing panels a and b in Figure 2, when similar fluorescence intensities were produced in the APF solution, the concentration of H_2O_2 was about 2000-fold greater than that of •OH.

APF was incubated with various concentrations of KO_2 solution to test its reactivity with $O_2^{\bullet-}$, and the increase in fluorescence intensity was shown in Figure 2c. The fluorescence response of APF to •OH was 180-fold greater than that of $O_2^{\bullet-}$, similar to the 200-fold increase in the literature.[29]

APF was incubated with various concentrations of EP solutions to test its reactivity with $^1O_2$, and the increase in fluorescence intensity was shown in Figure 2d. We found that APF response was about 120-fold greater to •OH than to $^1O_2$. These results coincide with the results in other papers.[29,30]

A strongly oxidizing species is required for the ipso-substitution reaction of APF.[29] Therefore, the different fluorescence responses of APF to ROS in Figure 1 are due to differences in the oxidizing powers of ROS. Using the different

DOI: 10.1021/acs.langmuir.6b01621
Langmuir 2016, 32, 11295−11302

fluorescence responses of APF to various ROS, we attempted to identify the ROS produced by NBs.

Identification of ROS Produced by Oxygen NB Water. *To Examine Whether the ROS Produced by NB Water Is H_2O_2.* H_2O_2 is cytotoxic but is considered a relatively weak oxidizing reagent (electrode potential: E (H_2O_2, H^+/•OH, H_2O) = 0.39 V). H_2O_2 is stable and has a long lifetime from hours to days in water. It can permeate into membranes and has a long lifetime within the cell. Here, we tried to verify whether H_2O_2 can be produced by NB water.

Figure 3 shows the effects of ferrous ions on the fluorescence intensities of NB and control water (baseline fluorescence by

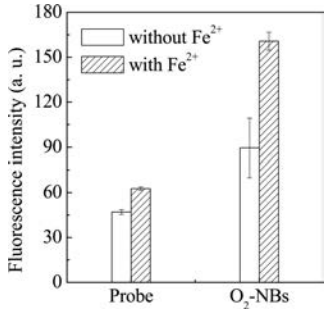

Figure 3. Effect of ferrous ion (20 μM) on the fluorescence intensities of the buffer solutions with and without NBs. Before ferrous ion was added, the fluorescence intensities of oxygen NB water (hollow column) were higher than control (probe, hollow column) by about 40. After ferrous ion was added, the fluorescence intensities of oxygen NB water (shaded column) and the probe (shaded column) increased by about 15 and 70, respectively.

probe). Before ferrous ions were added, the fluorescence intensities of oxygen NB water were statistically higher than those of control water. The fluorescence increase of the APF solution caused by oxygen NB water was approximately 40. According to the formula in Figure 2b, the oxidative capacity of oxygen NB water was equivalent to 0.5 mM H_2O_2. Similarly, the oxidative capacity of oxygen NB water was equivalent to 0.25 μM of •OH, 50 μM of $O_2^{\bullet-}$, or 30 μM of $^1O_2$ according to the formulas in Figure 2c,d. Thus, if the ROS produced by NBs is H_2O_2, the NB water should contain about 0.5 mM of H_2O_2.

According to the Fenton reaction shown in eq 1, in the presence of excess amounts of H_2O_2, the concentration of added ferrous ions is equal to that of •OH. As can be seen in Figure 2a, in the presence of 0.1 mM H_2O_2, the fluorescence intensity of APF increased substantially with the addition of ferrous sulfate in the range 0−25 μM. We supposed that 0.5 mM H_2O_2 existed in the NB water. Thus, after 20 μM of ferrous sulfate was added, 20 μM •OH should be produced. Compared to the values before 20 μM ferrous sulfate was added, the fluorescence intensities of NB water would increase by more than 2000. However, in Figure 3, after 20 μM ferrous sulfate was added, the fluorescence intensity of NB water increased only by about 70. Thus, we can conclude that the ROS produced by NBs was not H_2O_2.

From Figure 3, the fluorescence intensity of control water significantly increased by about 15 after 20 μM ferrous ions was added. The reason was considered to be as follows. According to eq 2, ferrous ions will react with dissolved oxygen and produce $O_2^{\bullet-}$. The concentration of the added ferrous ions was 20 μM. The dissolved oxygen concentration in the control water was about 8 mg/L (over 250 μM), which showed the excess in the reaction solution. Hence, 20 μM ferrous ion will produce 20 μM $O_2^{\bullet-}$. According to the equation in Figure 2c, when 20 μM $O_2^{\bullet-}$ is produced, the fluorescence increase should be about 15. The value in Figure 3 coincided with our calculated value from the correlation curve in Figure 2c.

$$Fe^{2+} + O_2 \rightarrow Fe^{3+} + O_2^{\bullet-} \quad (2)$$

To Examine Whether the ROS Produced by NB Water Is $O_2^{\bullet-}$. $O_2^{\bullet-}$ has two electrode potentials ($E(O_2/O_2^{\bullet-})$ = −0.35 V and $E(O_2^{\bullet-}, 2H^+/H_2O_2)$ = 0.91 V), showing that $O_2^{\bullet-}$ can act both as an oxidant and as a mild reductant.[31] Compared to other radicals, $O_2^{\bullet-}$ has a relatively long lifetime in the range of milliseconds to seconds,[32] which enables diffusion within the cell and thereby increases the number of the potential targets. In this section, we tried to verify whether $O_2^{\bullet-}$ could be produced by NB water.

From the results in Figure 2c and Figure 3, if the ROS produced by NBs is $O_2^{\bullet-}$, the NB water must contain about 50 μM of $O_2^{\bullet-}$. According to eq 3, the dismutation of 1 mol of $O_2^{\bullet-}$ catalytic with SOD will lead to the formation of 1/2 a mole of H_2O_2.[33] Thus, in the presence of 50 μM of $O_2^{\bullet-}$ in NB water, we can obtain about 25 μM H_2O_2. According to the formulas in Figure 2b, 25 μM of H_2O_2 will not cause a significant increase in the fluorescence intensity of APF.

$$O_2^{\bullet-} + O_2^{\bullet-} \xrightarrow{SOD} O_2 + H_2O_2 \quad (3)$$

Thus, after adding SOD to the NB water, the fluorescence intensity of NB water should be the same as that of the control water. When we add ferrous ions to the NB water, they will react with H_2O_2 to produce •OH according to eq 1. The fluorescence intensity of NB water will significantly increase.

To verify our hypothesis, we applied the above procedure to both the KO_2 solution and NB water. First, we prepared 0.1 M KO_2 stock solution. Immediately after the preparation, we added 30 μL of KO_2 solution to the buffer solutions of APF with and without 6 units of SOD. As the lifetime of $O_2^{\bullet-}$ was very short, the real concentration of $O_2^{\bullet-}$ was much lower than the theoretical concentration (0.3 mM). As can be seen in Figure 4a, after adding the KO_2 solution, the fluorescence

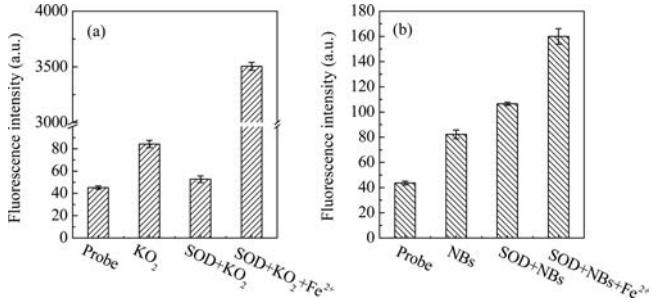

Figure 4. Effect of SOD (6 units) and ferrous ion on the fluorescence intensities of superoxide radical solution and NBs solutions.

increases of the buffer solutions of APF with and without 6 units SOD were about 7 and 40, respectively. According to Figure 2c, when the fluorescence increase was 40, the $O_2^{\bullet-}$ concentration in the APF solution should be 50 μM. Therefore, the real concentration of $O_2^{\bullet-}$ added to the APF solution was about 50 μM. Thus, 25 μM H_2O_2 was formed in the APF solution with 6 units of SOD. Then, excess amount of ferrous sulfate (30 μM) was added, and the fluorescence intensity

DOI: 10.1021/acs.langmuir.6b01621
Langmuir 2016, 32, 11295−11302

increased by about 3500, as shown in Figure 4a, which was consistent with the theoretical value. On the contrary, the fluorescence increases of NB water with and without 6 units SOD were 60 and 40, respectively (Figure 4b). In the presence of SOD, after adding ferrous sulfate (30 μM), the fluorescence intensity increased by only 120 (Figure 4b). These results offered clear evidence that the ROS produced by NBs was not $O_2^{\bullet-}$.

To Examine Whether the ROS Produced by NB Water Is •OH or $^1O_2$. •OH is the strongest oxidant and has a much higher electrode potential (E(•OH, H^+/H_2O) = 2.31 V) than the other ROS.[31] Due to its high reactivity and short lifetime, on the order of nanoseconds,[34] •OH's mobility range is extremely limited. It is not membrane permeable but can only react with surrounding molecules. $^1O_2$ has a short lifetime, about 2−4 μs,[35] but it is capable of diffusion and is permeate membranes. The electrode potential of $^1O_2$ is 0.81 V (E ($^1O_2/O_2^{\bullet-}$)). In this section, we tried to identity whether the ROS produced by NB water is •OH or $^1O_2$.

DMSO is known to quench •OH but not $^1O_2$.[30] Figure 5a shows the fluorescence response of APF to 4 μM •OH in the presence of different amounts of DMSO. Without DMSO, the fluorescence increase of APF caused by 4 μM •OH was about 530. After DMSO was added, the fluorescence intensities substantially decreased, as shown in Figure 5a. The fluorescence reaction of •OH with APF was quenched about 80% by 0.1% DMSO and about 95% by 0.2% DMSO. The quenching of •OH with APF by 1% DMSO was similar to that by 0.2% DMSO, which meant that DMSO above 0.2% did not have further effects on quenching. Since DMSO is toxic to cells, for safety concerns, a 0.2% concentration of DMSO was used in the following experiments. Figure 5b shows the fluorescence response of APF to 40 μM $^1O_2$ in the presence of 0.2% DMSO. $^1O_2$ was produced from EP powder which was dissolved in a buffer containing 10% ethanol. As shown in Figure 5b, 0.2% DMSO showed no quenching of APF fluorescence by $^1O_2$. The above results showed that 0.2% DMSO could suppress about 95% of APF fluorescence derived from •OH without affecting the signal derived from $^1O_2$.

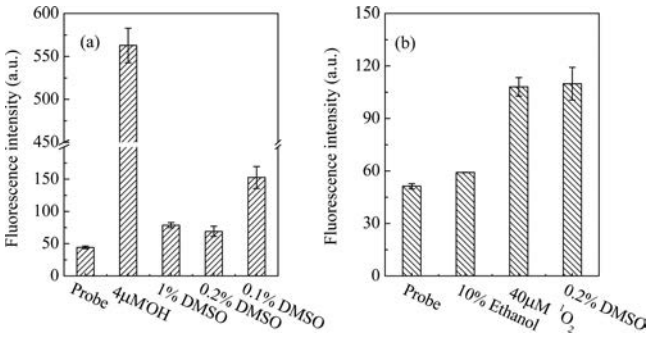

Figure 5. Effect of DMSO on the fluorescence intensities of hydroxyl radical solution and singlet oxygen solutions (a) The fluorescence response of APF to 4 μM •OH in the presence of different amount of DMSO. (b) The fluorescence response of APF to 40 μM $^1O_2$ in the presence of 0.2% DMSO. The •OH was formed by the Fenton reaction; the $^1O_2$ was formed by the EP powder dissolved in buffer solution containing 10% ethanol.

Then, we studied the effect of DMSO on the fluorescence response of APF to oxygen NB water. APF was added to the NB water with and without 0.2% DMSO, and then the fluorescence intensities of these NB waters were measured. As can be seen in Figure 6, without 0.2% DMSO, the fluorescence increase of APF solution caused by oxygen NB water was approximately 40. In the presence of 0.2% DMSO, the fluorescence intensities of NB water and control water (probe) showed no significant difference, meaning that DMSO quenched APF fluorescence by oxygen NB water. These results clearly showed that the ROS produced by NB water is •OH. According to the formulas in Figure 2a, oxygen NB water could produce about 0.25 μM of •OH.

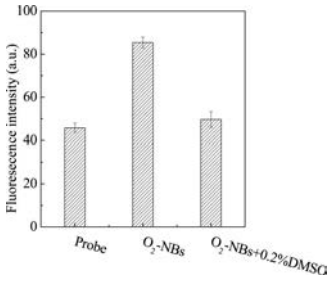

Figure 6. Effect of DMSO on the fluorescence intensities of oxygen NB water.

In a MNB generator, hydrodynamic cavitation may occur. It is widely known that hydrodynamic cavitation can generate •OH and also H_2O_2, whose concentrations are in the micro molar level.[36,37] Although micro molar level •OH may form during the MNB generation, it will immediately disappear due to the very short lifetime. The NB water we used in this paper was taken after we stopped the MNB generator. Thus, the •OH we observed was produced due to NBs themselves rather than MNB generator during the MNB generation process. Micromolar level of H_2O_2 can exist for a relatively long time. In Figure 3, after 20 μM ferrous sulfate was added, the fluorescence intensity of oxygen NB water increased by about 70. Based on the calculation from the formula in Figure 2a, it is possible that the fluorescence increase was due to the Fenton reaction between the existence of submicro molar level H_2O_2 and excess amount of ferrous sulfate. Although the micromolar H_2O_2 has almost no effect on the physiological activity of living organisms, the H_2O_2 may form the strongest oxidant •OH associated with the disappearance of NBs in the water. The research for •OH formation by NB water is worth doing in the near future.

Effect of NB Number Density on the Germination of Vegetable Seeds. Most of the previous studies have focused on analyzing the effect of exogenously added H_2O_2 on the seed physiology. Exogenous H_2O_2 stimulates the germination of dormant seeds of barley,[7] *Arabidopsis*,[38] rice,[9] and Zinnia elegans.[39] Other ROS such as •OH have been largely ignored because of their short lifetimes. As NB water can continually produce submicromolar levels of •OH[17] (Figures 2−6), it is possible to study the role of exogenously added •OH in the seed germination process.

We studied the role of exogenous •OH produced by NBs in the water in the seed-germination process. As the amount of •OH is positively correlated with the NB number density in water,[17] waters of two different NB number densities (100% NB water and 20% NB water) were prepared for germination tests, as described in the Experimental Section.

Figure 7a displays the germination rates of spinach seeds in response to different treatments at 20 °C. For spinach seed,

DOI: 10.1021/acs.langmuir.6b01621
Langmuir 2016, 32, 11295−11302

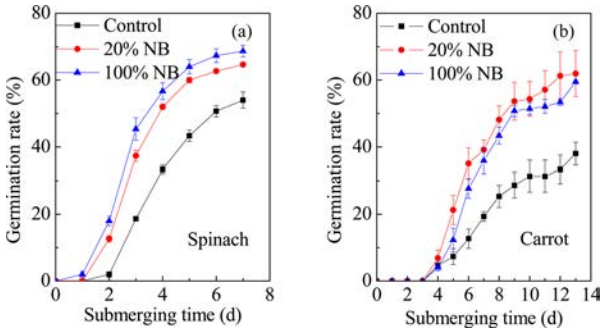

Figure 7. Effect of NB number density on the germination process of spinach seeds and carrot seeds. (a) Spinach seeds. (b) Carrot seeds. The error bars show the standard errors of three parallel samples.

visible radicle emergence was initiated within 1−2 days after submerging in 100% NB water and 20% NB water. However, for the seeds submerged in distilled water, the radicle emergence was delayed by 1 day. The final germination rates of spinach seeds in distilled water, 20% NB water, and 100% NB water were 54%, 65%, and 69%, respectively. Besides, 100% NB water can promote the growth of the sprout system. The sprout lengths of spinach seeds submerged in 100% NB water were longer than those submerged in the distilled water as shown in Figure 8a−c.

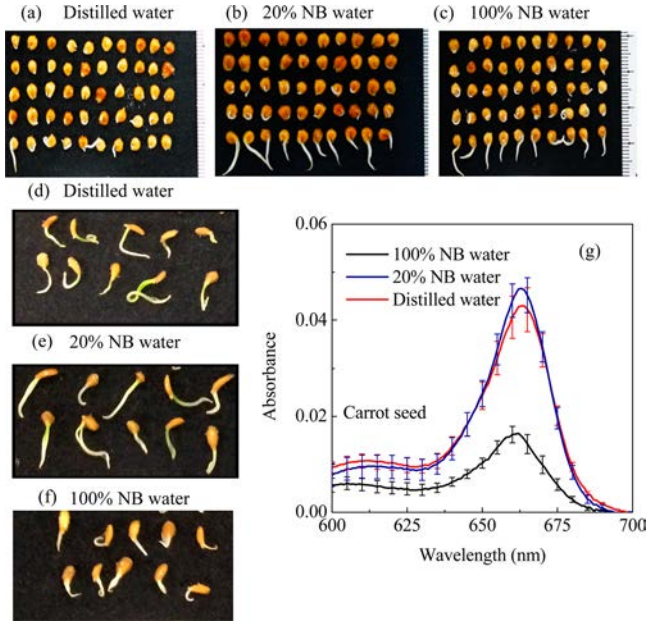

Figure 8. Effect of NB number density on the hypocotyl elongation and chlorophyll content of carrot seeds and spinach seeds. Fifty Spinach seeds are all shown in panels a−c. Ten carrot seeds in d−f are representatives of 50 seeds. (g) The absorbance of chlorophyll content of carrot seeds submerged in three kinds of waters. The error bars show the standard errors of three parallel samples.

Figure 7b shows the germination rates of carrot seeds in response to different treatments at 20 °C. The final germination rates of carrot seeds in distilled water, 20% NB water and 100% NB water were 38%, 62%, and 59%, respectively. However, for carrot seeds, the 100% NB water prohibited the elongation of radicles as seen in Figure 8d−f. The sprouts of carrot seeds dipped in 100% NB water were smaller than those in 20% NB water and distilled water. Moreover, the radicle did not turn green. On the final day of the germination tests, the chlorophyll contents of carrot seeds submerged in three groups were compared, as shown in Figure 8g. The absorbance value at 652 nm can be used to represent the chlorophyll content.[40] It is clear that the chlorophyll contents of carrot seeds submerged in 100% NB water were obviously lower than those in distilled water and 20% NB water. The low value of chlorophyll content can be thought as the negative effect caused by high-number density NB water.

The amount, duration, and localization are very important factors when we consider the role of ROS in physiological processes. At the nanomolar and submicromolar levels, ROS function as signaling molecules and are involved in regulation development and pathogen-defense responses.[41,42] At the micromolar level, ROS can promote adaptation and possibly organismal fitness. They are also involved in signal transduction pathways in association with ROS-induced apoptosis and necrosis.[1,43] At the millimolar or higher, ROS will cause irreversible damage to cellular compounds.

In NB water, the amount of •OH is at the submicromolar level, and is beneficial to cell growth and viability. However, the oxidative window for carrot seeds we used in our experiments is very narrow. The amount of exogenous •OH produced by 100% NB water was beyond the toxic threshold of carrot seeds, thus showing inhibition of the elongation of the hypocotyl.

SUMMARY AND CONCLUSIONS

Using a sensitive fluorescent probe APF, we established a set of methods to distinguish the four major types of ROS and identified the specific type of ROS using oxygen NB water. We found clear evidence that NB water can produce submicromolar •OH in water. Together with the identification of the ROS generated by NBs, we have found that NB water with different bubble-number densities had different effects on the germination processes of spinach and carrot seeds. The amount of exogenous •OH has a positive correlation with the NB number density in the water. High-number density NB water (i.e., above 1×10^8 particles/mL) led to the higher final germination rates and faster germination processes for spinach seeds. However, for carrot seeds, the same high-number density NB water was beyond the toxic threshold and inhibited the elongation of the hypocotyl and the chlorophyll formation. When the NB water was diluted, the relatively low number density of NB water (2×10^7 particles/mL) did not show any negative effects while promoting the germination of carrot seeds.

As the toxic thresholds for each type of seeds are different, the usage of NB water should be judged individually for each target. Our study should inspire further work on the many roles of NB water in both sterilization processes and growth promotion for living organisms. To gain a deeper understanding of NB water's impact on living organisms, molecular biological and genomic research should also be done in the future.

ASSOCIATED CONTENT

Supporting Information

The Supporting Information is available free of charge on the ACS Publications website at DOI: 10.1021/acs.langmuir.6b01621.

Bubble size distribution in the 100 % NBs water and 20% NB water (PDF)

DOI: 10.1021/acs.langmuir.6b01621
Langmuir 2016, 32, 11295−11302

AUTHOR INFORMATION

Corresponding Authors

*Seiichi Oshita, E-mail: aoshita@mail.ecc.u-tokyo.ac.jp; TEL: 03-5841-5362; FAX: 03-5841-8174.

*Shu Liu, E-mail: liushu0313055@gmail.com.

Notes

The authors declare no competing financial interest.

ACKNOWLEDGMENTS

A part of this research has been financially supported by Challenging Exploratory Research (25660202); a Grant in Aid for Scientific Research (2402408) by JSPS; the Council for Science, Technology and Innovation (CSTI); the Cross-ministerial Strategic Innovation Promotion Program (SIP); "Technologies for creating next-generation agriculture, forestry and fisheries" (funding agency: Bio-oriented Technology Research Advancement Institution, NARO), Japan; and the Mayekawa Houonkai Foundation in 2015.

REFERENCES

(1) Hamanaka, R. B.; Chandel, N. S. Chandel. Mitochondrial reactive oxygen species regulate cellular signaling and dictate biological outcomes. *Trends Biochem. Sci.* **2010**, *35*, 505−513.

(2) Brieger, K.; Schiavone, S.; Miller, F. J., Jr; Krause, K. H. Reactive oxygen species: from health to disease. *Swiss Med. Wkly.* **2012**, *142*, w13659.

(3) Bailly, C.; El-Maarouf-Bouteau, H.; Corbineau, F. From intracellular signaling networks to cell death: the dual role of reactive oxygen species in seed physiology. *C. R. Biol.* **2008**, *331*, 806−814.

(4) Finkel, T. Signal transduction by reactive oxygen species. *J. Cell Biol.* **2011**, *194*, 7−15.

(5) Trachootham, D.; Lu, W. Q.; Ogasawara, M. A.; Valle, N. R. D.; Huang, P. Redox regulation of cell survival. *Antioxid. Redox Signaling* **2008**, *10* (8), 1343−1374.

(6) Apel, K.; Hirt, H. Reactive oxygen species: metabolism, oxidative stress, and signal transduction. Annu. *Annu. Rev. Plant Biol.* **2004**, *55*, 373−99.

(7) Ishibashi, Y.; Tawaratsumida, T.; Zheng, S. H.; Yuasa, T.; Iwaya-Inoue, M. NADPH Oxidases act as key enzyme on germination and seeding growth in barley (Hordeum vulgare L.). *Plant Prod. Sci.* **2010**, *13*, 45−52.

(8) Lariguet, P.; Ranocha, P.; De Meyer, M.; Barbier, O.; Penel, C.; Dunand, C. Identification of a hydrogen peroxide signalling pathway in the control of light-dependent germination in Arabidopsis. *Planta* **2013**, *238*, 381−395.

(9) Naredo, M. E. B.; Juliano, A. B.; Lu, B. R.; De Guzman, F.; Jackson, M. T. Responses to seed dormancy-breaking treatments in rice species (Oryza L.). *Seed Sci. Technol.* **1998**, *26*, 675−689.

(10) Park, J.; Kurata, K. Application of microbubbles to hydroponics solution promotes lettuce growth. *HortTechnology* **2009**, *19*, 212−215.

(11) Liu, S.; Kawagoe, Y.; Makino, Y.; Oshita, S. Effects of nanobubbles on the physicochemical properties of water: the basis for peculiar properties of water containing nanobubbles. *Chem. Eng. Sci.* **2013**, *93*, 250−256.

(12) Ebina, K.; Shi, K.; Hirao, M.; Hashimoto, J.; Kawato, Y.; Kaneshiro, S.; et al. Oxygen and air nanobubble water solution promote the growth of plants, fishes, and mice. *PLoS One* **2013**, *8*, e65339.

(13) Ohnari, H. Fisheries experiments of cultivated shells using micro-bubbles techniques. *J. Heat Transfer Society Jpn.* **2001**, *40*, 2−7 (In Japanese).

(14) Ohnari, H.; Ohnari, H.; Nakayama, T.; Nakata, A.; Yamamoto, T. Generating mechanism of microbubble and its physiological characteristics. *Visualization Society of Japan* **2003**, *23*, 105−106 (in Japanese).

(15) Weber, J.; Agblevor, F. A. Microbubble fermentation of Trichoderma reesei for cellulase production. *Process Biochem.* **2005**, *40*, 669−676.

(16) Matsuno, H.; Ohta, T.; Shundo, A.; Fukunaga, Y.; Tanaka, K. Simple surface treatment of cell-culture scaffolds with ultrafine bubble water. *Langmuir* **2014**, *30*, 15238−15243.

(17) Liu, S.; Oshita, S.; Makino, Y.; Wang, Q. H.; Kawagoe, Y.; Uchida, T. Oxidative Capacity of Nanobubbles and Its Effect on Seed Germination. *ACS Sustainable Chem. Eng.* **2016**, *4*, 1347−1353.

(18) Minamikawa, K.; Takahashi, M.; Makino, T.; Tago, K.; Hayatsu, M. Irrigation with oxyen-nanobubble water can reduce methane emission and arsenic dissolution in a flooded rice paddy. *Environ. Res. Lett.* **2015**, *10*, 084012.

(19) Kalyanaraman, B.; Darley-Usmar, V.; Davies, K. J.; Dennery, P. A.; Forman, H. J.; Grisham, M. B.; Mann, G. E.; Moore, K.; Roberts, L. J., 2nd; Ischiropoulos, H. Measuring reactive oxygen and nitrogen species with fluorescent probes: challenges and limitations. *Free Radical Biol. Med.* **2012**, *52*, 1−6.

(20) Kranner, I.; Roach, T.; Beckett, R. P.; Whitaker, C.; Minibayeva, F. V. Extracellular production of reactive oxygen species during seed germination and early seedling growth in Pisumsativum. *J. Plant Physiol.* **2010**, *167*, 805−811.

(21) Takahashi, M.; Ishikawa, H.; Asano, T.; Horibe, H. Effect of microbubbles on ozonized water for photoresist removal. *J. Phys. Chem. C* **2012**, *116*, 12578−12583.

(22) Takahashi, M.; Chiba, K.; Li, P. Formation of hydroxyl radicals by collapsing ozone microbubbles under strongly acidic conditions. *J. Phys. Chem. B* **2007**, *111*, 11443−11446.

(23) Li, P.; Takahashi, M.; Chiba, K. Enhanced free-radical generation by shrinking microbubbles using a copper catalyst. *Chemosphere* **2009**, *77*, 1157−1160.

(24) Povich, M. J. Measurement of dissolved oxygen concentrations and diffusion coeffieients by electron spin resonance. *Anal. Chem.* **1975**, *47* (2), 346−347.

(25) Tada, K.; Maeda, M.; Nishiuchi, Y.; Nagahara, J.; Hata, T.; Zhuowei, Z.; Yoshida, Y.; Watanabe, S.; Ohmori, M. ESR Measurement of Hydroxyl Radicals in Micro-nanobubble Water. *Chem. Lett.* **2014**, *43*, 1907−1908.

(26) Gomes, A.; Fernandes, E.; Lima, J. L. F. C. Fluorescence probes used for detection of reactive oxygen species. *J. Biochem. Biophys. Methods* **2005**, *65*, 45−80.

(27) Hempel, S. L.; Buettner, G. R.; O'Malley, Y. Q.; Wessels, D. A.; Flaherty, D. M. Dihydrofluorescein diacetate is superior for detecting intracellular oxidants: comparison with 2′,7′-dichlorodihydrofluorescein diacetate, 5(and 6)-carboxy-2′,7′-dichlorodihydrofluorescein diacetate, and dihydrorhodamine 123. *Free Radical Biol. Med.* **1999**, *27*, 146−159.

(28) Fenton, H. J. H. Oxidation of tartaric acid in the presence of iron. *J. Chem. Soc., Trans.* **1894**, *65*, 899−910.

(29) Setsukinai, K.-i.; Urano, Y.; Kakinuma, K.; Majima, H. J.; Nagano, T. Development of novel fluorescence probes that can reliably detect reactive oxygen species and distinguish specific species. *J. Biol. Chem.* **2003**, *278*, 3170−3175.

(30) Price, M.; Reiners, J. J.; Santiago, A. M.; Kessel, D. Monitoring singlet oxygen and hydroxyl radical formation with fluorescent probes during photodynamic therapy. *Photochem. Photobiol.* **2009**, *85* (5), 1177−1181.

(31) Koppenol, W. H.; Stanbury, D. M.; Bounds, P. L. Electrode potentials of partially reduced oxygen species, from dioxygen to water. *Free Radical Biol. Med.* **2010**, *49*, 317−322.

(32) Chen, X. J.; West, A. C.; Cropek, D. M.; Banta, S. Detection of the Superoxide Radical Anion Using Various Alkanethiol Monolayers and Immobilized Cytochrome c. *Anal. Chem.* **2008**, *80*, 9622−9629.

(33) McCord, J. M.; Fridovich, I. Superoxide dismutase. An enzymic function for erythrocypein (Hemocuprein). *J. Biol. Chem.* **1969**, *244* (22), 6049−6055.

(34) Donoghue, M. A.; Xu, X.; Bernlohr, D. A.; Arriaga, E. A. Capillary electrophoretic analysis of hydroxyl radicals produced by respiring mitochondria. *Anal. Bioanal. Chem.* **2013**, *405*, 6053−6060.

DOI: 10.1021/acs.langmuir.6b01621
Langmuir 2016, 32, 11295−11302

(35) Lindig, B. A.; Rodgers, M. A. J.; Schaap, A. P. Determination of the lifetime of singlet oxygen in water-d2 using 9,10-anthracenedipropionic acid, a water-soluble probe. *J. Am. Chem. Soc.* **1980**, *102*, 5590−5593.
(36) Chakinala, A. G.; Gogate, P. R.; Burgess, A. E.; Bremner, D. H. Industrial wastewater treatment using hydrodynamic cavitation and heterogeneous advanced Fenton processing. *Chem. Eng. J.* **2009**, *152*, 498−502.
(37) Arrojo, S.; Nerin, C.; Benito, Y. Application of salicylic acid dosimetry to evaluate hydrodynamic cavitation as an advanced oxidation process. *Ultrason. Sonochem.* **2007**, *14*, 343−349.
(38) Lariguet, P.; Ranocha, P.; De Meyer, M.; Barbier, O.; Penel, C.; Dunand, C. Identification of a hydrogen peroxide signalling pathway in the control of light-dependent germination in Arabidopsis. *Planta* **2013**, *238* (2), 381−95.
(39) Ogawa, K.; Iwabuchi, M. A mechanism for promoting the germination of Zinnia seeds by hydrogen peroxide. *Plant Cell. Physiol.* **2001**, *42*, 286−291.
(40) Root, R. A.; Miller, R. J.; Koeppe, D. E. Uptake of cadmium—Its toxicity, and effect on the iron ratio in hydroponically Grown Corn. *J. Environ. Qual.* **1973**, *4*, 473−476.
(41) Burch, P. M.; Heintz, N. H. Redox regulation of cell-cycle reentry: cyclin D1 as a primary target for the mitogenic effects of reactive oxygen and nitrogen species. *Antioxid. Redox Signaling* **2005**, *7*, 741−751.
(42) Kim, M. J.; Johnson, W. A. ROS-mediated activation of drosophila larval nociceptor neurons by UVC irradiation. *BMC Neurosci.* **2014**, *15*, 14.
(43) Day, R. M.; Suzuki, Y. J. Cell proliferation, reactive oxygen and cellular glutathione. *Dose-Response* **2005**, *3*, 425−442.

DOI: 10.1021/acs.langmuir.6b01621
Langmuir 2016, 32, 11295−11302